

Short Papers

Optimum Codesign for Image Denoising Between Type-2 Fuzzy Identifier and Matrix Completion Denoiser

Qi Liu [✉], Member, IEEE, Xiaopeng Li [✉], and Jicheng Yang

Abstract—With the wide deployment of digital image capturing equipment, the need of denoising to produce a crystal clear image from noisy capture environment has become indispensable. In this article, a novel type-2 fuzzy-based filter is proposed for denoising images corrupted by impulse noise, especially for the high density of salt-and-pepper noise. It operates two stages, namely, type-2 fuzzy identifier and matrix completion denoiser. In the proposed method, the type-2 fuzzy identifier is first employed to identify and trim the entries contaminated by impulse noise in the data matrix from fuzzy system. Then, the trimmed data matrix is utilized to retrieve the noiseless data matrix with the matrix completion technology. Herein, a novel matrix completion technique is developed without *a priori* rank information compared to its counterparts. Simulation results are presented, which vividly show the denoised images obtained by the proposed method can achieve crystal clear image with strong structural integrity, and are showing good performance in terms of peak signal-to-noise ratio.

Index Terms—Gaussian noise, image denoising, matrix completion, salt-and-pepper noise, type-2 fuzzy identifier.

I. INTRODUCTION

Image denoising, as one of the most fundamental and important tasks in image processing, has spurred on-going interests in machine learning and computer vision [1]. It is because the natural image is inevitably corrupted by impulse noise during phases of acquisition and transmission, such as electrical conditions, light intensity, and imperfection in imaging sensors. They are the major sources of this noise degrading the image quality in the subsequent image processing applications, including object segmentation, edge detection, feature extraction [2], [3], and to name just a few.

The tradeoff between suppressing the noise and preserving the sharpness of edge and detail information, is the objective of noise removal. In the weighted nuclear norm minimization (WNNM) algorithm [4], the low-rank regularization is enforced to reconstruct the latent structure of the noisy patch matrix. However, it only considers the nonlocal self-similarity property of the noise corrupted image, which makes it difficult to denoise the image from the noisy observation alone. The nonlinear filtering techniques, including standard median filter (MF) [5], center weight median filter (CWMF) [6], adaptive weighted median filter (AWMF) [7], and truncated median filter (TMF) [8], have been demonstrated to be superior to linear filtering (moving average) in suppressing impulse noise. However, the median filter tends to blur fine details and destroy edges while removing out the impulse noise.

Manuscript received March 12, 2020; revised July 5, 2020; accepted October 5, 2020. Date of publication October 13, 2020; date of current version December 31, 2021. (Corresponding author: Xiaopeng Li.)

Qi Liu and Jicheng Yang are with the Department of Electrical and Computer Engineering, National University of Singapore, 119077 Singapore, Singapore (e-mail: elelqi@nus.edu.sg; eleyji@nus.edu.sg).

Xiaopeng Li is with the Department of Electrical Engineering, City University of Hong Kong 999077, Hong Kong (e-mail: x.p.li.frank@gmail.com).

Digital Object Identifier 10.1109/TFUZZ.2020.3030498

The success of fuzzy techniques spurs numerous researchers to study fuzzy filters for image denoising [9], and the underlying reason is that the extra degree of fuzziness provides a more efficient way of handling uncertainty, which is inevitably encountered in noisy environment. These fuzzy filters, such as FIRE filter [10], weighted fuzzy mean filter [11], and fuzzy c-means clustering filter (FRFCM) [12], are able to outperform rank-order filter schemes, e.g., median filters. Nevertheless, the drawbacks of them rely on many external parameters heuristically determined by the users, including noise density and pixel weighting factors, that are not consistent to give satisfactory result for different noise levels. Moreover, it is hard to determine the optimal set of parameters. To address that, an adaptive type-2 fuzzy filter in [13] (which here is referred to as type-2 fuzzy) with a combination of type-1 fuzzy set, is proposed to eliminate the problems of fuzzy rule base matrix formation, fuzzification, and defuzzification. It seems that during denoising the bad pixels, however, the assignment of weight to good pixels in filtering window using inverse distance weighting function is vulnerable to small perturbation (e.g., Gaussian noise) to preserve the image details. In addition, type-2 fuzzy also succeed to be used in image edge detection [3], [14] with promising performance.

In this article, to overcome the aforementioned problems, codesign for image denoising between type-2 fuzzy identifier and matrix completion denoiser is developed, which is a two-steps approach—the first step involves the detection of pixels corrupted by impulse noise, followed by the second step of denoising those pixels. In the type-2 fuzzy identifier, bad pixels are detected and trimmed, which results in the problem of matrix completion. Then, a novel matrix completion technique without *a priori* knowledge of rank information in second step is devised to denoise images. This article makes notable contributions summarized as follows:

- 1) To the best of our knowledge, a pioneering idea is proposed by combining the matrix completion technique with type-2 fuzzy identifier. On the basis of type-2 fuzzy set with membership function, it is modified to identify and trim the pixels contaminated by impulse noise, which leads to solving the matrix completion problem. Therefore, based on the general framework, a family of matrix completion-based methods can be exploited, where the concept of matrix completion is commonly used in the application of image inpainting instead of image denoising.
- 2) A novel matrix completion approach is devised to involve in image denoising, where its parameter tuning-free property outperforms the existing matrix completion-based methods with predefined rank.
- 3) The proposed method not only works well on high density of salt-and-pepper noise, but also can successfully denoise the mixed noises, namely, salt-and-pepper and Gaussian noises. Simulation results verify the effectiveness of the proposed method

compared with the state-of-the-art fuzzy filters and well-known image denoisers. The code of this work is available at <https://sites.google.com/site/qiliucityu/discussion>.

II. PROPOSED METHOD

Consider a noisy grayscale image \mathbf{M} of size $n_1 \times n_2$ contaminated with additive noise, \mathbf{M}_{ij} represents the luminance value of pixel at location (i, j) , where $1 \leq i \leq n_1$ and $1 \leq j \leq n_2$ denote the row and column indices, respectively. The proposed method is composed of two-step operations, namely, a type-2 fuzzy identifier and a matrix completion denoiser.

A. Type-2 Fuzzy Identifier

For each pixel \mathbf{M}_{ij} at location (i, j) in the image, let a neighborhood region $[\mathbf{W}_H]_{i,j} \in \mathbb{R}^{(2H+1) \times (2H+1)}$ denote the group of pixels contained in a filtering window centered at location (i, j) of the noisy image, defined as follows:

$$[\mathbf{W}_H]_{i,j} = \mathbf{M}_{i+p,j+q}, \quad (p, q) \in \{-H, \dots, H\} \quad (1)$$

where H is the window half-size parameter.

The type-2 fuzzy sets and systems, characterized by the fuzzy membership functions (MFs), namely, primary and secondary MFs, have been proved that their extra degrees of fuzziness provide a powerful tool to handle those inevitably encountered uncertainties in noisy environments [15], [16]. Motivated by that, the Gaussian membership function (GMF) is introduced as follows:

$$m_{\mathcal{M}}(\mathbf{M}_{ij}) = e^{-(\mathbf{M}_{ij} - \mu_{ij}^{(H,\chi)}) / 2(\sigma_{ij}^{(H,\chi)})^2} \quad (2)$$

where \mathcal{M} denotes a fuzzy set characterized by GMF. Here, the parameters $\mu_{ij}^{(H,\chi)}$ and $\sigma_{ij}^{(H,\chi)}$ for GMF are defined as $\mu_{ij}^{(H,\chi)} = \mathcal{K}_{\chi}([\mathbf{W}_H]_{i,j})$ and $\sigma_{ij}^{(H,\chi)} = \mathcal{K}_{\chi}([\mathbf{A}_H]_{ij})$, $\chi = 1, \dots, h$, respectively. $\mathcal{K}_{\chi}(\cdot)$ stands for the mean of k -middle, also known as α -trimmed mean, defined as [13], [17]

$$\mathcal{K}_{\ell}(\mathcal{S}) = \begin{cases} \frac{1}{2\chi-1} \sum_{h-\chi+1}^{h+\chi-1} s_{\ell}, & \text{if } D \text{ is odd } (D = 2h - 1) \\ \frac{1}{2\chi} \sum_{h-\chi+1}^{h+\chi} s_{\ell}, & \text{if } D \text{ is even } (D = 2h) \end{cases} \quad (3)$$

where s_{ℓ} is the ℓ th element in set $\mathcal{S} = \{s_1, \dots, s_D\}$, h is the length of the filter window, and $[\mathbf{A}_H]_{ij}$ is computed by the absolute deviation between s_{ℓ} and $\mu = \frac{1}{h} \sum_{\chi=1}^h \mu_{ij}^{(H,\chi)}$. On that basis, the type-2 fuzzy identifier is defined as follows:

$$\varrho(\mathbf{M}_{ij}) = \begin{cases} \mathbf{M}_{ij}, & \text{if } \mathcal{K}_{\chi}(|s_{\ell} - \mu|) \geq T \\ 0, & \text{otherwise} \end{cases} \quad (4)$$

where T is a thresholding parameter based on the Gaussian membership values of the set \mathcal{S} [12].

Then, the novel data matrix with missing entries (bad pixels) is reconstructed as follows:

$$\mathbf{M}_{\Omega} := \begin{bmatrix} \varrho(\mathbf{M}_{11}) & \cdots & \varrho(\mathbf{M}_{1n_2}) \\ \vdots & \ddots & \vdots \\ \varrho(\mathbf{M}_{n_11}) & \cdots & \varrho(\mathbf{M}_{n_1n_2}) \end{bmatrix}. \quad (5)$$

The task is transformed to complete the matrix \mathbf{M}_{Ω} from noisy measurements. Therefore, a family of matrix completion techniques can be utilized, but most of them are based on the ideal assumption of known rank information, which is in general impractical. Next, to overcome

that, a novel matrix completion method is proposed without *a priori* rank information.

B. Matrix Completion Denoiser

Consider the matrix $\mathbf{M} \in \mathbb{R}^{n_1 \times n_2}$ of rank r , whose compact singular value decomposition (SVD) is given by $\mathbf{M} = \mathbf{U}\mathbf{\Sigma}\mathbf{V}^T := \sum_{i \in \mathbb{N}_r^+} \sigma_i(\mathbf{M}) \mathbf{u}_i \mathbf{v}_i^T$ with column and row subspaces, respectively, denoted as \mathbf{U} and \mathbf{V} , spanned by the sets $\{\mathbf{u}_i \in \mathbb{R}^{n_1 \times 1}\}_{i \in \mathbb{N}_r^+}$ and $\{\mathbf{v}_i \in \mathbb{R}^{n_2 \times 1}\}_{i \in \mathbb{N}_r^+}$, respectively. Let $\mathbf{M}_{\Omega} \in \mathbb{R}^{n_1 \times n_2}$ be a matrix with missing entries (bad pixels), where Ω is a subset of the complete set of entries $[n_1] \times [n_2]$ with $[n]$ being the list $\{1, \dots, n\}$. Throughout this article, the subscript $(\cdot)_{\Omega}$ represents the projection on the known entries. The (i, j) entry of \mathbf{M}_{Ω} , denoted by $[\mathbf{M}_{\Omega}]_{ij}$, can be written as follows:

$$[\mathbf{M}_{\Omega}]_{ij} = \begin{cases} \mathbf{M}_{ij}, & \text{if } (i, j) \in \Omega \\ 0, & \text{otherwise.} \end{cases} \quad (6)$$

The task of matrix completion is to find a matrix $\mathbf{X} \in \mathbb{R}^{n_1 \times n_2}$ given incomplete observation \mathbf{M}_{Ω} by incorporating the low-rank information. Mathematically, it is formulated as a rank minimization problem

$$\begin{aligned} \min_{\mathbf{X}} \quad & \text{rank}(\mathbf{X}) \\ \text{s.t.} \quad & [\mathbf{X}]_{ij} = [\mathbf{M}]_{ij}, \quad (i, j) \in \Omega. \end{aligned} \quad (7)$$

Unfortunately, the rank minimization problem is NP-hard in general since the rank is highly discrete and nonconvex. To handle this issue, nuclear norm minimization is proposed to relax rank minimization [18], which is analogous to the strategy of approximation of ℓ_0 -norm replaced by ℓ_1 -norm in compressed sensing [19]. Therefore, it results in a nuclear norm optimization problem

$$\begin{aligned} \min_{\mathbf{X}} \quad & \|\mathbf{X}\|_* \\ \text{s.t.} \quad & [\mathbf{X}]_{ij} = [\mathbf{M}]_{ij}, \quad (i, j) \in \Omega \end{aligned} \quad (8)$$

where $\|\mathbf{X}\|_* := \sum_r \sigma_r$ denotes the nuclear norm of matrix \mathbf{X} . Numerous state-of-the-art approaches have been proposed to deal with the nuclear norm optimization problem in (8). Nevertheless, most of them require the rank information and full SVD operation. It is impractical to know *a priori* rank information. Moreover, the full SVD operation will result in a demanding computational complexity. To save the computational burden without SVD operation, matrix factorization has been exploited, corresponding to the following optimization problem [20]:

$$\min_{\mathbf{U}, \mathbf{V}} \|\mathbf{M}_{\Omega} - (\mathbf{U}\mathbf{V})_{\Omega}\|_F^2 \quad (9)$$

where $\mathbf{U} \in \mathbb{R}^{n_1 \times r}$ and $\mathbf{V} \in \mathbb{R}^{r \times n_2}$ with r being the rank of target matrix. Nevertheless, (9) is difficult to address because of its nonconvexity. One may solve the problem (9) in an iterative manner as a biconvex problem, \mathbf{U} and \mathbf{V} are alternately minimized as follows:

$$\begin{cases} \mathbf{V}^{t+1} = \arg \min_{\mathbf{V}} \|\mathbf{M}_{\Omega} - (\mathbf{U}^t \mathbf{V})_{\Omega}\|_F^2 \\ \mathbf{U}^{t+1} = \arg \min_{\mathbf{U}} \|\mathbf{M}_{\Omega} - (\mathbf{U} \mathbf{V}^{t+1})_{\Omega}\|_F^2 \end{cases} \quad (10)$$

Then, the target matrix can be computed by $\mathbf{M} = \mathbf{U}^{t+1} \mathbf{V}^{t+1}$ after determining \mathbf{U} and \mathbf{V} , which is due to the fact that the low-rank property of \mathbf{X} is automatically fulfilled with *a priori* rank in each iteration.

Motivated by that, we devise a simple but efficient matrix completion method based on ℓ_2 -norm, where the ℓ_2 -norm of matrix \mathbf{E} is defined as $\|[\mathbf{E}]_{ij}\|_2^2 = \sum_{i,j} |[\mathbf{E}]_{ij}|^2$, $(i, j) \in \Omega$. At first, we consider that a decision matrix \mathbf{X} is decomposed as a summation of a set of rank-one

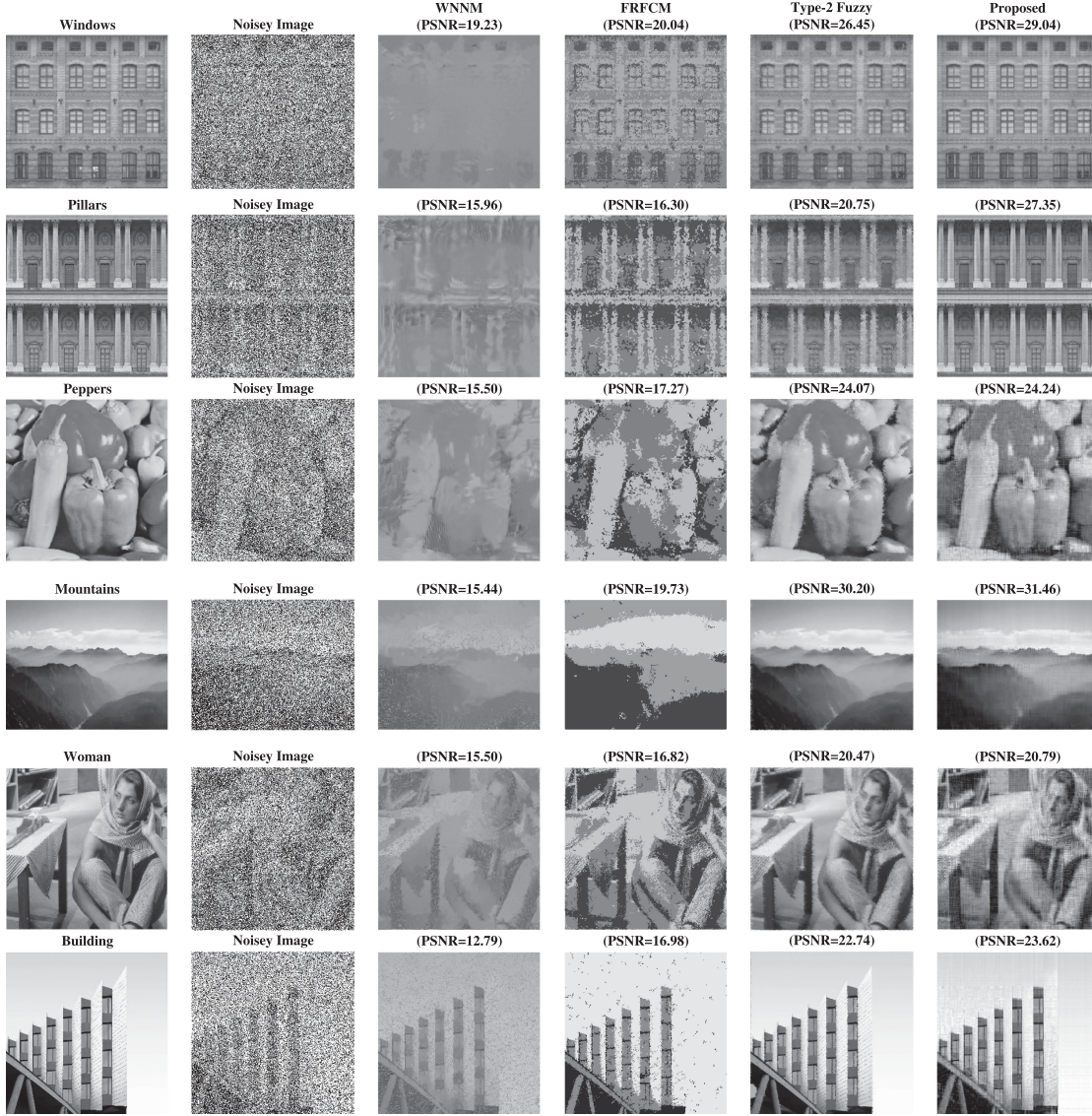


Fig. 1. First column: Six original grayscale images are used to examine the denoising performance, namely, *Windows*, *Pillars*, *Peppers*, *Mountains*, *Woman*, and *Building*. Second column: Noisy images with 0.65 density of salt-and-pepper noise. Followed by the denoising results of WNNM [4], FRFCM [12], Type-2 Fuzzy [13] and the proposed method in each columns, respectively.

matrices, that is

$$\mathbf{X} = \sum_{\ell=1}^q \mathbf{X}_{\ell} \quad (11)$$

where $\mathbf{X}_{\ell} = \mathbf{u}_{\ell} \mathbf{v}_{\ell}^T$. Combining with (11) and (9) is equivalently transformed into

$$\min_{\mathbf{X}} \left\| \mathbf{M}_{\Omega} - \left(\sum_{\ell=1}^q \mathbf{X}_{\ell} \right) \right\|_{\Omega}^2 \quad (12)$$

To be more specific, it results in

$$\mathcal{G} : \min_{\mathbf{u}, \mathbf{v}} \left\| [\mathbf{M}]_{ij} - \left[\sum_{\ell=1}^q \mathbf{u}_{\ell} \mathbf{v}_{\ell}^T \right]_{ij} \right\|_{\Omega}^2, \quad (i, j) \in \Omega. \quad (13)$$

Let us define the block $\mathbf{Y} := (\mathbf{Y}_1, \dots, \mathbf{Y}_{2q}) = (\{\mathbf{u}_{\ell}^q\}_{\ell=1}, \{\mathbf{v}_{\ell}^q\}_{\ell=1})$. From the analysis in [21], block coordinate descent (BCD) method can

converge to a critical point when the following conditions are satisfied:

$$\tilde{\mathcal{G}}_{\ell}(\mathbf{Y}_{\ell} | \mathbf{Y}_{-\ell}^{\ell-1}) = \mathcal{G}(\mathbf{Y}_{\ell} | \mathbf{Y}_{-\ell}^{\ell-1}) \quad (14)$$

$$\tilde{\mathcal{G}}_{\ell}(\mathbf{Y}_{\ell} | \mathbf{Y}_{-\ell}) \leq \mathcal{G}(\mathbf{Y}_{\ell} | \mathbf{Y}_{-\ell}), \forall \mathbf{Y}_{-\ell} \quad (15)$$

$$\nabla \tilde{\mathcal{G}}_{\ell}(\mathbf{Y}_{\ell} | \mathbf{Y}_{-\ell}^{\ell-1}) = \nabla \mathcal{G}(\mathbf{Y}_{\ell} | \mathbf{Y}_{-\ell}^{\ell-1}) \quad (16)$$

$$\tilde{\mathcal{G}}_{\ell}(\mathbf{Y}_{\ell} | \mathbf{Y}_{-\ell}^{\ell-1}) \text{ is continuous in } \mathbf{Y}. \quad (17)$$

where $\tilde{\mathcal{G}}(\{\mathbf{u}_{\ell}^q\}_{\ell=1}, \{\mathbf{v}_{\ell}^q\}_{\ell=1})$ is the surrogate function of $\mathcal{G}(\{\mathbf{u}_{\ell}^q\}_{\ell=1}, \{\mathbf{v}_{\ell}^q\}_{\ell=1})$. Following the rational of BCD method, we define the surrogate function as:

$$\tilde{\mathcal{G}} : \min_{\mathbf{u}_q, \mathbf{v}_q} \left\| \mathbf{R}_q - [\mathbf{u}_q \mathbf{v}_q^T]_{ij} \right\|_{\Omega}^2, \quad (i, j) \in \Omega \quad (18)$$

for each q th iteration, where $\mathbf{R}_q := \mathbf{M}_{\Omega} - (\sum_{\ell=1}^{q-1} \mathbf{u}_{\ell} \mathbf{v}_{\ell}^T)_{\Omega}$ with $q \geq 2$ and $\mathbf{R}_1 = \mathbf{M}_{\Omega}$. For each \mathbf{Y}_{ℓ} , $\ell = 1, \dots, 2q$, it is easy to observe that the least squares (LS) problem in (18) is convex when the others

TABLE I
COMPARISON OF THE PROPOSED METHOD WITH STATE-OF-THE-ART FUZZY FILTERS AND WELL-KNOWN
IMAGE DENOISERS IN DIFFERENT RATIOS OF SALT-AND-PEPPER NOISE

Image	Density	MF [5]	TMF [8]	AWMF [7]	WNNM [4]	FRFCM [12]	Type-2 Fuzzy [13]	Proposed
<i>Windows</i>	10%	35.07	24.54	24.51	23.98	25.19	42.08	33.73
	20%	29.43	24.30	24.28	22.88	24.61	38.50	33.49
	30%	23.96	23.76	24.00	21.97	24.61	35.46	33.20
	40%	19.24	21.91	23.52	21.07	24.04	32.54	32.70
	50%	15.52	17.00	23.52	20.11	23.17	29.89	32.17
	60%	12.66	12.01	23.52	19.53	21.54	29.88	31.23
	70%	10.33	12.01	23.52	19.05	18.20	25.35	30.08
	80%	8.45	7.13	23.52	17.73	8.97	23.16	28.29
90%	6.94	6.36	23.52	15.94	6.31	20.86	25.19	
<i>Pillars</i>	10%	24.87	19.70	19.67	21.23	21.07	32.85	31.50
	20%	23.17	19.39	19.47	20.21	20.70	29.56	31.00
	30%	20.41	18.97	19.17	19.29	20.26	27.27	30.51
	40%	17.54	17.28	18.78	18.28	19.55	25.19	29.73
	50%	14.46	15.22	17.97	17.27	18.52	23.43	29.13
	60%	11.94	11.66	16.00	16.47	17.22	21.58	28.04
	70%	9.83	8.921	13.15	15.49	14.82	19.82	26.77
	80%	7.98	7.20	9.91	14.42	8.89	18.33	25.34
90%	6.60	6.24	7.36	13.28	6.14	16.69	20.68	
<i>Peppers</i>	10%	33.27	20.45	20.44	24.03	22.64	41.64	32.36
	20%	28.20	20.32	20.36	22.71	22.46	37.76	31.21
	30%	23.23	20.32	20.24	21.17	22.25	34.44	30.04
	40%	18.57	20.32	19.97	19.69	21.74	31.38	28.84
	50%	15.15	16.78	19.14	18.49	20.98	28.29	27.14
	60%	12.15	12.80	16.97	17.26	19.34	25.55	25.64
	70%	9.94	9.54	13.56	16.00	15.78	22.94	22.97
	80%	8.04	7.65	10.17	14.43	9.44	20.24	20.92
90%	6.57	6.38	7.34	13.14	6.24	17.29	17.61	
<i>Mountains</i>	10%	37.10	24.52	24.53	30.43	21.23	43.93	35.54
	20%	30.56	24.52	24.48	26.46	21.21	41.22	35.17
	30%	23.78	24.31	24.39	23.36	21.19	38.63	34.33
	40%	18.66	24.31	24.11	20.71	21.11	35.83	33.85
	50%	15.04	19.23	22.26	18.31	20.94	33.84	33.06
	60%	11.90	14.29	18.122	16.50	20.24	31.58	32.05
	70%	9.50	14.29	13.80	14.70	17.88	28.97	30.57
	80%	7.68	8.06	10.04	13.16	9.39	26.32	28.38
90%	6.15	6.30	7.09	11.55	5.95	23.30	24.90	
<i>Woman</i>	10%	28.73	19.72	19.70	23.82	20.59	36.59	26.14
	20%	25.77	19.54	19.56	22.40	20.38	33.22	25.88
	30%	21.67	19.24	19.56	20.78	20.14	30.66	25.58
	40%	17.90	18.41	19.56	19.20	19.75	28.48	25.17
	50%	14.58	16.05	18.34	17.63	19.15	26.50	24.60
	60%	11.79	12.53	16.21	16.28	17.97	24.19	23.81
	70%	9.56	9.50	12.95	17.80	15.22	22.61	22.67
	80%	7.71	7.53	12.95	13.35	8.57	20.48	20.79
90%	6.25	6.19	12.95	12.02	6.03	17.63	18.23	
<i>Building</i>	10%	28.42	21.91	21.94	26.64	20.97	28.45	24.80
	20%	25.65	21.91	21.79	23.65	20.77	27.74	24.79
	30%	21.40	21.33	21.58	20.61	20.59	26.88	24.60
	40%	17.33	20.49	21.18	17.99	20.30	25.90	24.24
	50%	13.73	18.22	19.85	15.72	19.70	24.76	24.04
	60%	11.00	18.22	16.57	13.67	18.49	23.45	23.73
	70%	8.71	10.89	12.66	12.00	14.91	21.90	23.30
	80%	6.87	8.08	9.07	10.54	7.98	20.11	22.29
90%	5.36	5.90	6.19	9.24	5.38	17.59	20.31	

are fixed. Therefore, the conditions from (14) to (17) are satisfied. At the ℓ th iteration, variable Υ_ℓ , $\ell = 1, \dots, 2q$, is updated by solving the following problem:

$$\Upsilon_\ell^\ell = \arg \min_{\Upsilon_\ell} \tilde{G}_\ell(\Upsilon_\ell | \Upsilon_{-\ell}^{\ell-1}) \quad (19)$$

with respect to block variable Υ_ℓ , and $\Upsilon_{-\ell}^{\ell-1}$ represents the rest of the variables obtained at the $(\ell - 1)$ th iteration except for Υ_ℓ . Instead of optimizing the original objective function, we alternatively optimize a surrogate function $\tilde{G}_\ell(\Upsilon_\ell | \Upsilon_{-\ell}^{\ell-1})$, which satisfies certain requirements such that the original problem can be easily tackled.

Toward this end, we utilize the greedy pursuit manner to search for the best rank-one basis matrix of the current residual \mathbf{R}_q and the iteratively reweighted least squares (IRLS) method [22] is employed to tackle the problem (18) in a BCD manner [21]. To be specific, based on the rationale of alternating minimization, we fix variable \mathbf{v} and then optimize \mathbf{u} , resulting in

$$\mathbf{u}_q^\ell = \arg \min_{\mathbf{u}_q} \left\| \mathbf{R}_q - [\mathbf{u}_q(\mathbf{v}_q^{\ell-1})^T]_{ij} \right\|_2^2, \quad (i, j) \in \Omega. \quad (20)$$

Support that \mathbf{r}_i and u_i are the i th row of \mathbf{R}_q and i th entry of \mathbf{u}_q , respectively. As $\{\mathbf{r}_i\}_{i=1}^{n_1}$ are independent for each u_i , (20) is equivalent

to tackling the following n_1 independent subproblems:

$$u_i^\ell = \arg \min_{u_i} \|\mathbf{r}_i - u_i(\mathbf{v}_i^{\ell-1})^T\|_2^2, \quad (i, j) \in \Omega. \quad (21)$$

Since $\mathbf{R}_q = \mathbf{M}_\Omega - (\sum_{\ell=1}^{q-1} \mathbf{u}_\ell \mathbf{v}_\ell^T)_\Omega$ and $\mathbf{r}_i = [\mathbf{R}_q]_i$ is the i th row of \mathbf{R}_q , it is easily observed that the residual error in (21) is only affected by all non-zero elements in \mathbf{r}_i and $u_i(\mathbf{v}_i^{\ell-1})^T$. Therefore, (21) is further simplified as follows:

$$u_i^\ell = \arg \min_{u_i} \|\ddot{\mathbf{r}}_i - u_i(\ddot{\mathbf{v}}_i^{\ell-1})^T\|_2^2 \quad (22)$$

where $\ddot{\mathbf{r}}_i$ and $\ddot{\mathbf{v}}_i^{\ell-1}$ stand for the \mathbf{r}_i and $\mathbf{v}_i^{\ell-1}$ with nonzero entries inside, respectively. The problem (22) is easily handled as it is a LS problem. To guarantee the solution of (22) to perform good performance, IRLS is utilized, which can provide global convergence. In the optimization problem of IRLS, it addresses a weighted LS problem as follows:

$$(u_i^\ell)^{t+1} = \arg \min_{(u_i^\ell)^t} \|\ddot{\mathbf{r}}_i - (u_i^\ell)^t \ddot{\mathbf{v}}_i^{\ell-1})^T \mathbf{w}^t\|_2^2 \quad (23)$$

where $w_i^t = 1/(\max\{\delta, |(\ddot{\mathbf{r}}_i - (u_i^\ell)^t \ddot{\mathbf{v}}_i^{\ell-1})^T\})$ is the i th element of \mathbf{w}^t , and $(u_i^\ell)^t$ is initialized at $(u_i^\ell)^0 = (\ddot{\mathbf{v}}_i^{\ell-1})^T \ddot{\mathbf{r}}_i / ((\ddot{\mathbf{v}}_i^{\ell-1})^T \ddot{\mathbf{v}}_i^{\ell-1})$. Thus, δ is a small regularization value, e.g., 10^{-3} , to avoid dividing by zero. Toward this end, the solution of block $\{\mathbf{u}\}_{\ell=1}^q$ has been achieved.

Taking in similar manner, we update \mathbf{v} by fixing \mathbf{u} .

$$\mathbf{v}_q^\ell = \arg \min_{\mathbf{v}_q} \|\mathbf{R}_q - [\mathbf{u}_q^\ell \mathbf{v}_q^T]_{ij}\|_2^2, \quad (i, j) \in \Omega. \quad (24)$$

Then, we have its simplified version with non-zeros, namely

$$(v_j^\ell)^{t+1} = \arg \min_{(v_j^\ell)^t} \|\ddot{\mathbf{r}}_j - (\ddot{\mathbf{u}}_j^\ell)^{t+1} (v_j^\ell)^t\|_2^2, \quad (i, j) \in \Omega. \quad (25)$$

where $\ddot{\mathbf{r}}_j$ and $\ddot{\mathbf{u}}_j^\ell$ denote the j th column of \mathbf{R}_q and \mathbf{u}_j^ℓ after removing missing entries, respectively.

III. SIMULATIONS

In this section, the denoising performance of the proposed method is investigated in terms of peak signal-to-noise ratio (PSNR) [23], to provide quality evaluation. The six standard grayscale images with different sizes, including *Windows* (508×481), *Pillars* (300×300), *Peppers* (317×316), *Mountains* (500×400), *Woman* (817×817) and *Building* (1080×1080). For each test image, we perform the experiments for different levels of corruption by salt-and-pepper noise, from 10% to 90% with scale of 10%. Our simulations are performed using MATLAB R2015b on a system with 3.40 GHz intel core i7 CPU and 4 GB RAM, under a 64-bit Windows 7 operating system.

In the first experiment, we examine the denoising performance of the proposed method with comparison to the state-of-the-art fuzzy filters FRFCM [12] and type-2 fuzzy [13], and well-known image denoisers WNNM [4], as shown in Fig. 1. The density of salt-and-pepper noise is 0.65. From Fig. 1, it is observed that the proposed method achieves the highest PSNR on six test images and is superior to the compared approaches in the cases of test images with strong structural integrity. In Table I, the quantitative results of MF [5], TMF [8], AWMF [7], WNNM [4], FRFCM [12], and Type-2 Fuzzy [13] are compared with the proposed method, where the salt-and-pepper noise level is varied from 10% to 90%. For comparative analysis, the proposed method and type-2 fuzzy method are more effective to eliminate the noise and both of them provide higher PSNR than others. Thus, the Type-2 Fuzzy method performs better at low level of salt-and-pepper noise, however,

TABLE II
COMPARISON OF THE PROPOSED METHOD WITH THE TYPE-2 FUZZY FILTER IN THE MIXED NOISE

Image	Density	Type-2 Fuzzy	Proposed
<i>Windows</i>	20%	18.02	24.05
	50%	16.24	23.95
	80%	14.84	21.86
<i>Pillars</i>	20%	15.70	21.30
	50%	15.59	20.28
	80%	14.86	17.48
<i>Peppers</i>	20%	16.61	20.01
	50%	16.18	19.86
	80%	15.04	18.29
<i>Mountains</i>	20%	17.39	20.55
	50%	16.20	20.40
	80%	15.08	19.43
<i>Woman</i>	20%	16.44	19.20
	50%	15.91	19.16
	80%	14.96	17.88
<i>Building</i>	20%	15.36	17.53
	50%	15.33	17.23
	80%	14.86	16.12

it is inferior to the proposed method with high density of salt-and-pepper noise.

To further demonstrate the effectiveness of the proposed method, noise removal in mixed noises, namely, salt-and-pepper and Gaussian noises, is investigated for image denoising, where the Gaussian noise is distributed with zero mean and variance of 0.05. The results of three different ratios of salt-and-pepper noise, viz. 20%, 50%, and 80%, are presented in Table II. In the case of mixed noises even with Gaussian noise mean as low as 0.05, the denoising performance of the type-2 fuzzy filter degrade significantly in terms of PSNR. It makes sense because the rationale of type-2 fuzzy filter is that good retained pixels are utilized to weight to bad pixels. Nevertheless, in the mixed noises, those ‘‘good’’ pixels are corrupted by Gaussian noise. In addition, the proposed method outperforms the type-2 fuzzy filter at around 6 dB for images with strong structural integrity, and at approximately 3 dB for other test images.

IV. CONCLUSION

In this article, a new and effective image denoising approach was proposed with the combination of type-2 fuzzy identifier and matrix completion denoiser. With the help of type-2 fuzzy identifier, bad pixels were identified and trimmed, leading to an incomplete matrix with missing entries. Then, a novel matrix completion technique without *a priori* rank information is developed as the denoiser. Compared with the state-of-the-art fuzzy filters, the proposed method achieves the best denoising performance on test images with strong structural integrity, and more superior PSNR than others for high density of salt-and-pepper noise. What is more, the proposed method also enjoys satisfactory denoising performance in the mixed noises. For the future study, however, the design of more computationally efficient matrix completion denoiser merits further investigation.

ACKNOWLEDGMENT

The authors would like to thank the handling editor and anonymous reviewers for their constructive feedback.

REFERENCES

- [1] P. K. Saha, S. Basu, and E. A. Hoffman, "Multiscale opening of conjoined fuzzy objects: Theory and applications," *IEEE Trans. Fuzzy Syst.*, vol. 24, no. 5, pp. 1121–1133, Oct. 2016.
- [2] K. Cao, E. Liu, and A. K. Jain, "Segmentation and enhancement of latent fingerprints: A coarse to fine ridgestructure dictionary," *IEEE Trans. Pattern Anal. Mach. Intell.*, vol. 36, no. 9, pp. 1847–1859, Sep. 2014.
- [3] P. Melin, C. I. Gonzalez, J. R. Castro, O. Mendoza, and O. Castillo, "Edge-detection method for image processing based on generalized type-2 fuzzy logic," *IEEE Trans. Fuzzy Syst.*, vol. 22, no. 6, pp. 1515–1525, Dec. 2014.
- [4] S. Gu, L. Zhang, W. Zuo, and X. Feng, "Weighted nuclear norm minimization with application to image denoising," in *Proc. IEEE Conf. Comput. Vis. Pattern Recognit.*, Columbus, OH, USA, Jun. 2014, pp. 2862–2869.
- [5] T. Nodes and N. Gallagher, "Median filters: Some modifications and their properties," *IEEE Trans. Acoust., Speech, Signal Process.*, vol. 30, no. 5, pp. 739–746, Oct. 1982.
- [6] S. Ko and Y. H. Lee, "Center weighted median filters and their applications to image enhancement," *IEEE Trans. Circuits Syst.*, vol. 38, no. 9, pp. 984–993, Sep. 1991.
- [7] T. Loupas, W. N. McDicken, and P. L. Allan, "An adaptive weighted median filter for speckle suppression in medical ultrasonic images," *IEEE Trans. Circuits Syst.*, vol. 36, no. 1, pp. 129–135, Jan. 1989.
- [8] E. Davies, "On the noise suppression and image enhancement characteristics of the median, truncated median and mode filters," *Pattern Recognit. Lett.*, vol. 7, no. 2, pp. 87–97, 1988.
- [9] V. P. Ananthi, P. Balasubramaniam, and P. Raveendran, "Impulse noise detection technique based on fuzzy set," *IET Signal Process.*, vol. 12, no. 1, pp. 12–21, 2018.
- [10] F. Russo and G. Ramponi, "A fuzzy operator for the enhancement of blurred and noisy images," *IEEE Trans. Image Process.*, vol. 4, no. 8, pp. 1169–1174, Aug. 1995.
- [11] C.-S. Lee, Y.-H. Kuo, and P.-T. Yu, "Weighted fuzzy mean filters for image processing," *Fuzzy Sets Syst.*, vol. 89, no. 2, pp. 157–180, 1997.
- [12] T. Lei, X. Jia, Y. Zhang, L. He, H. Meng, and A. K. Nandi, "Significantly fast and robust fuzzy c-means clustering algorithm based on morphological reconstruction and membership filtering," *IEEE Trans. Fuzzy Syst.*, vol. 26, no. 5, pp. 3027–3041, Oct. 2018.
- [13] V. Singh, R. Dev, N. K. Dhar, P. Agrawal, and N. K. Verma, "Adaptive type-2 fuzzy approach for filtering salt and pepper noise in grayscale images," *IEEE Trans. Fuzzy Syst.*, vol. 26, no. 5, pp. 3170–3176, Oct. 2018.
- [14] C. I. Gonzalez, P. Melin, J. R. Castro, O. Castillo, and O. Mendoza, "Optimization of interval type-2 fuzzy systems for image edge detection," *Appl. Soft Comput.*, vol. 47, pp. 631–643, 2016.
- [15] C. Lee, M. Wang, and H. Hagrais, "A type-2 fuzzy ontology and its application to personal diabetic-diet recommendation," *IEEE Trans. Fuzzy Syst.*, vol. 18, no. 2, pp. 374–395, Apr. 2010.
- [16] A. Niewiadomski, "On finity, countability, cardinalities, and cylindrical extensions of type-2 fuzzy sets in linguistic summarization of databases," *IEEE Trans. Fuzzy Syst.*, vol. 18, no. 3, pp. 532–545, Jun. 2010.
- [17] F. Ahmed and S. Das, "Removal of high-density salt-and-pepper noise in images with an iterative adaptive fuzzy filter using alpha-trimmed mean," *IEEE Trans. Fuzzy Syst.*, vol. 22, no. 5, pp. 1352–1358, Oct. 2014.
- [18] J.-F. Cai, E. J. Candès, and Z. Shen, "A singular value thresholding algorithm for matrix completion," *SIAM J. Optim.*, vol. 20, no. 4, Jan. 2010, Art. no. 1956–1982.
- [19] Q. Liu, C. Yang, Y. Gu, and H. C. So, "Robust sparse recovery via weakly convex optimization in impulsive noise," *Signal Process.*, vol. 152, pp. 84–89, 2018.
- [20] W. Zeng and H. C. So, "Outlier-robust matrix completion via ℓ_p -minimization," *IEEE Trans. Signal Process.*, vol. 66, no. 5, pp. 1125–1140, Mar. 2018.
- [21] M. Razaviyayn, M. Hong, and Z. Luo, "A unified convergence analysis of block successive minimization methods for nonsmooth optimization," *SIAM J. Optim.*, vol. 23, pp. 1126–1153, 2012.
- [22] D. P. O'Leary, "Robust regression computation using iteratively reweighted least squares," *SIAM J. Matrix Anal. Appl.*, vol. 11, no. 3, May 1990, Art. no. 466–480.
- [23] Z. Wang, A. C. Bovik, H. R. Sheikh, and E. P. Simoncelli, "Image quality assessment: From error visibility to structural similarity," *IEEE Trans. Image Process.*, vol. 13, no. 4, pp. 600–612, Apr. 2004.